2010

At the foot of the shrew: manus morphology distinguishes closely-related *Cryptotis goodwini* and *Cryptotis griseoventris* (Mammalia: Soricidae) in Central America

Neal Woodman
USGS Patuxent Wildlife Research Center, woodmann@si.edu

Ryan B. Stephens
University of Wisconsin

The Linnean Society of London BIOLOGICAL Journal of the Linnean Society

Biological Journal of the Linnean Society, 2010, **99**, 118–134. With 7 figures

At the foot of the shrew: manus morphology distinguishes closely-related *Cryptotis goodwini* and *Cryptotis griseoventris* (Mammalia: Soricidae) in Central America

NEAL WOODMAN[1]* and RYAN B. STEPHENS[2]

[1]*USGS Patuxent Wildlife Research Center, National Museum of Natural History, Smithsonian Institution, Washington, DC 20013, USA*
[2]*Department of Biology, University of Wisconsin, Stevens Point, WI 31030, USA*

Received 22 May 2009; accepted for publication 29 July 2009

Small-eared shrews (Mammalia, Soricidae) of the New World genus *Cryptotis* are distributed from eastern North America to the northern Andes of South America. One well-defined clade in this genus is the Central American *Cryptotis mexicana* group, whose members are set off from other species in the genus by their variably broader fore feet and more elongate and broadened fore claws. Two species in the *C. mexicana* group, *Cryptotis goodwini* Jackson and *Cryptotis griseoventris* Jackson, inhabit highlands in Guatemala and southern Mexico and are presumed to be sister species whose primary distinguishing feature is the larger body size of *C. goodwini*. To better characterize these species and confirm the identification of recently-collected specimens, we obtained digital X-ray images of the manus from large series of dried skins of both species. Measurements of the metacarpals and phalanges successfully separated most specimens of *C. goodwini* and *C. griseoventris*. These measurements also show that the fore feet of *C. griseoventris* from Chiapas, Mexico, are morphologically distinct from those of members of the species inhabiting Guatemala. Univariate, bivariate, and multivariate analyses indicate that fore foot characters are more conservative within species of the *C. mexicana* group than are cranio-mandibular characters. Patterns of evolution of fore foot characters that superficially appear to be linear gradations are actually more complex, illustrating individual evolutionary trajectories.

ADDITIONAL KEYWORDS: anatomy – digit – Insectivora – manus – ray – skeleton – small-eared shrew – Soricinae – Soricomorpha.

INTRODUCTION

Small-eared shrews (Mammalia, Soricidae) of the New World genus *Cryptotis* occur from the eastern USA and southernmost Canada through Central America to the northern Andes of South America. Recent taxonomic treatments typically partition the species among four morphological groups that likely represent clades (Woodman & Pefaur, 2008). The best-defined of these groups is the *Cryptotis mexicana* group, whose members inhabit highland regions of Mexico and northern Central America (Woodman, 2005). Among the distinguishing features of the *C. mexicana* group are notably enlarged fore feet and lengthened and broadened fore claws. These external modifications of the fore foot are associated skeletally with a more robust and complex humerus; shortened and broadened metacarpals, proximal phalanges, and middle phalanges; and lengthened and broadened distal phalanges of the manus (Woodman & Timm, 1999). To varying degrees, many of these same modifications mark the evolution of the talpid fore limb (Reed, 1951), and have been interpreted as enhancing digging ability for the more derived members of the *C. mexicana* group (Woodman & Timm, 1999).

*Corresponding author. E-mail: woodmann@si.edu

A previous investigation of the fore foot morphology of small-eared shrews documented extensive variation with distinct morphological patterns distinguishing some clades within the genus (Woodman & Morgan, 2005). Although taxon sampling was incomplete, the fore feet of individual species were sufficiently differentiated that they could be distinguished based on the relative proportions of the metacarpal and phalanges associated with digit III of the manus. Three species representing the *C. mexicana* group [*Cryptotis goldmani* (Merriam), *Cryptotis goodwini* Jackson, *C. mexicana* (Coues)] displayed a regular pattern of increased length of distal phalanx, length of claw, and breadth of metacarpals and phalanges with increased body size (Woodman & Morgan, 2005) that complemented patterns of variation previously documented for the humerus in this group (Woodman & Timm, 1999, 2000).

Recent field work in the highlands of Guatemala has provided additional specimens of small-eared shrews of the *C. mexicana* group and provided the opportunity to make a more focused examination of two species within this clade. *Cryptotis goodwini* and *Cryptotis griseoventris* Jackson currently are recognized as occurring in southern Chiapas, Mexico, and Guatemala. The two shrews are considered to be closely related (likely sister species) and are poorly differentiated. The primary characteristic used to distinguish them has been the larger size of *C. goodwini*; however, cranial measurements of the two species overlap broadly (Woodman & Timm, 1999; Woodman & Croft, 2005). Because differences in the fore foot skeleton have been documented among other members of the *C. mexicana* group, we attempted to characterize the morphology of the manus within these two species, initially as a means of assisting in their identification. Traditional preparations generally do not include post-cranial skeletons, so relatively few skeletons of these shrews are preserved in systematic collections, making it difficult to study skeletal characteristics. Traditional methods of preparing dried skins, however, typically preserve the articulated skeleton of the manus with the skin. We used a digital X-ray system to image and study these bones. In the present study, we report on the structure of the fore foot skeleton of these shrews and quantify the variation that we observed. We focus our attention on variability in the relative proportions of the metacarpals and phalanges, particularly those associated with the middle digit, because these bones are most consistently available to measure, and they have been useful for both discriminating species in previous studies of the manus of shrews (Woodman & Timm, 1999, 2000; Woodman & Morgan, 2005) and identifying functional groups among mammals (Weisbecker & Schmid, 2007; Kirk *et al.*, 2008).

MATERIAL AND METHODS

In the present study, we use the term 'ray' for parts of the manus associated with the metacarpal and the phalanges and the term 'digit' to refer to those portions associated with just the phalanges.

We X-rayed either the left (preferred) or right manus of dried skins of shrews using a Kevex-Varian digital X-ray system set at 36 kV, 0.099 mA in the Division of Fishes, Department of Vertebrate Zoology, National Museum of Natural History, Washington, DC. Digital images were transferred to Adobe Photoshop CS3 (version 10.0.1; Adobe Systems Inc.), trimmed, converted to positive images, and saved (Fig. 1). We quantified variation in the metacarpals, phalanges, and external claws of rays I, III, and V of the manus by measuring images of these elements with the custom Measurement Scale in the Analysis menu of Photoshop CS3. The scale was calibrated with a metal straight pin of known width (0.52 mm) included in each image. The measurements (with their abbreviations) recorded were (Fig. 2): CL = length of claw; CW = width of claw; DPL = length of distal phalanx; DPW = width of distal phalanx; ML = length of metacarpal; MPL = length of middle phalanx; MPW = width of middle phalanx; MW = width of metacarpal; P2L = length of proximal two bones of ray I (= ML + PPL); P2W = combined widths of proximal two bones of ray I; P3L = length of proximal three bones of ray III or V (= ML + PPL + MPL); P3W = combined widths of proximal three bones of ray III or V; PPL = length of proximal phalanx; PPW = width of proximal phalanx; TL = total length of ray (= ML + PPL + MPL + DPL); TW = total width of all bones of ray (= MW + PPW + MPW + DPW). All measurements are in given in millimetres and are rounded to the nearest 0.01 mm. Length of head and body (HB) in mm, calculated from external measurements recorded by collectors, was used as a proxy for body size. Tabled univariate statistics include the mean ± SD and total range. All statistical analyses were carried out in SYSTAT, version 11.00.01 (Systat Software, Inc.).

To compare variation among variables having different means, we calculated unbiased coefficients of variation (V^*; Sokal & Rohlf, 1981). To gauge intensities of associations among variables, we calculated pairwise Pearson's product-moment correlations (see Appendix I). Strong correlations were considered to be indicated by coefficients > 0.75. To understand how individual bones varied within and among populations relative to size of the manus, we calculated three sets of percentages: (1) the length of each bone divided by total length of the proximal two bones (P2L) for ray I or three bones (P3L) for rays III and V; (2) the width of each individual bone divided by its

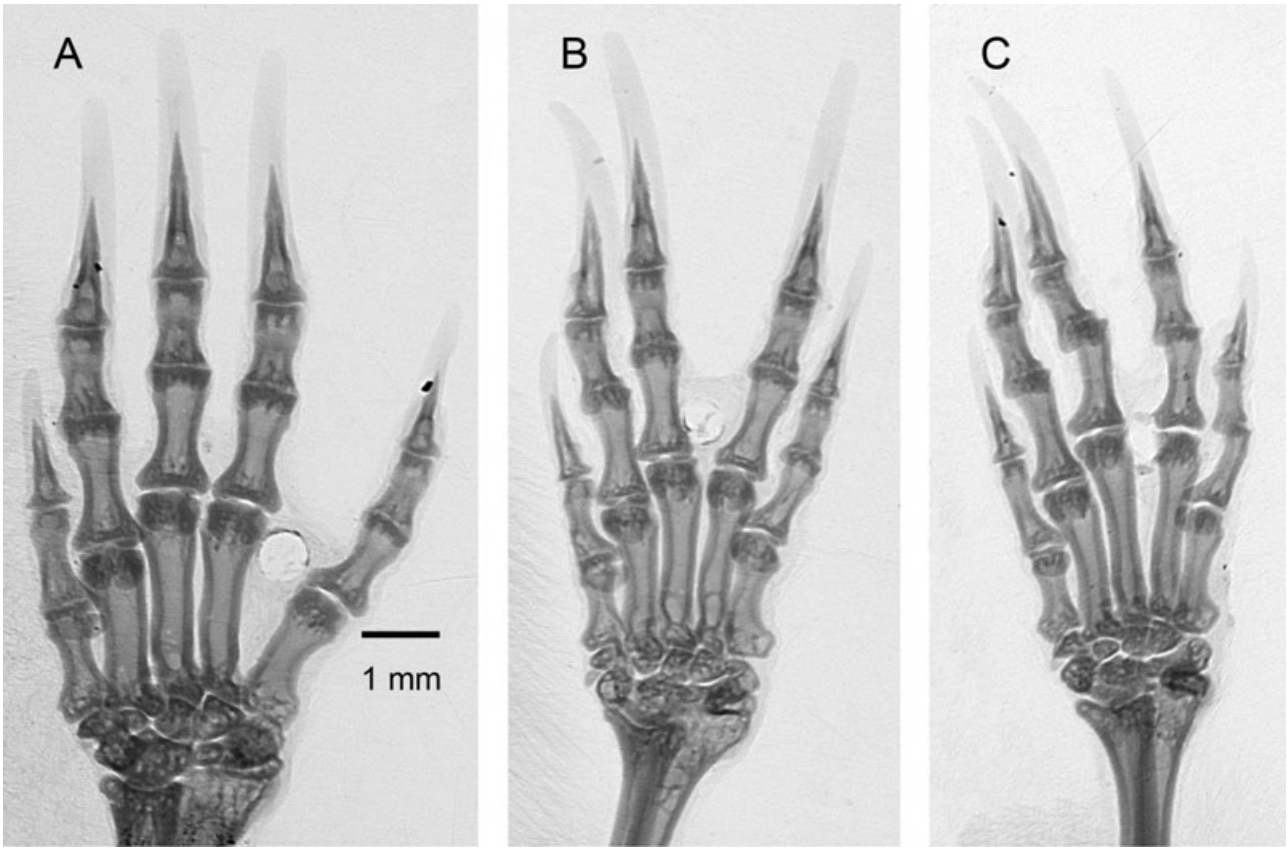

Figure 1. Digital X-rays of the right manus of specimens. A, *Cryptotis goodwini* (USNM 77078). B, the Todos Santos population (USNM 77057). C, *Cryptotis griseoventris* (USNM 75890). Original negatives were converted to positive images. All images are shown to the same scale.

length, which provides a gauge of relative shortening and/or widening; (3) the phalangeal index (PI), which yields proportional lengths of individual digits (i.e. PPL + MPL) relative to their metapodials. For rays III and V, PI = [(MPL + PPL)/ML × 100]; for ray I, PI = [PPL/ML × 100]. The PI is a morphological proxy used to infer differential substrate use within and among specific mammalian groups, especially in attempts to reconstruct functional morphology of fossil mammals (Lemelin, 1999; Weisbecker & Schmid, 2007; Kirk *et al.*, 2008). Because enlargements of the fore foot and fore claws among members of the *C. mexicana* group have been interpreted as adaptations to enhance digging ability (Woodman & Timm, 1999), we wanted to determine how these shrews would group with respect to other terrestrial and fossorial mammals. A second means of relating manus morphology to substrate is by plotting the relative proportions of the metacarpal, proximal phalanx, and middle phalanx of ray III on ternary diagrams (Kirk *et al.*, 2008). A third method is by determing relative lengths of the rays (Lemelin, 1999), calculated by dividing rays I and V by the longest ray, ray III.

We used principal components analysis (PCA) to characterize overall variation in morphology among all specimens as a group. Our PCA used a correlation matrix of seven log-transformed variables (DPL, DPW, MPL, MPW, PPL, PPW, ML) from ray III, the ray that showed the greatest variation among the three groups. To explore the cohesion of populations and our ability to distinguish them, we performed discriminant function analysis. Beginning with the same seven log-transformed variables, we employed both a backward stepwise procedure (beginning with all variables and removing individual variables from the model) and a forward stepwise procedure (beginning with no variables, then adding individual variables), each with alpha-to-enter and alpha-to-remove of 0.150.

Specimens examined in the present study are listed in Appendix II. Among these are three large series collected in 1895–1896 (Jackson, 1933; Goldman, 1951) that make up the bulk of known specimens of

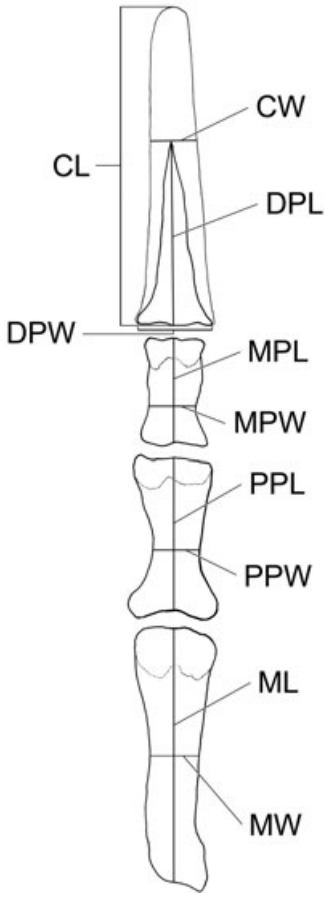

Figure 2. Dorsal view of ray III from the right manus of *Cryptotis goodwini*, illustrating measurements used in the present study. CL, length of claw; CW, width of claw; DPL, length of distal phalanx; DPW, width of distal phalanx; ML, length of metacarpal; MPL, length of middle phalanx; MPW, width of middle phalanx; MW, width of metacarpal; PPL, length of proximal phalanx; PPW, width of proximal phalanx.

these species: (1) the type series of *C. goodwini* from Calel, Guatemala; (2) the type series of *C. griseoventris* from San Cristóbal de las Casas, Chiapas, Mexico; (3) a second large sample of *C. griseoventris* from Todos Santos Cuchumatán, Guatemala, approximately 160 km south-east of the type locality. Early in the study, we realized that the fore foot morphology of the two samples of *C. griseoventris* are distinct. This finding was unexpected because the two populations are otherwise difficult to distinguish (Woodman & Timm, 1999). We subsequently included the Guatemalan representatives of this species as a separate sample, designated informally as 'Todos Santos'. We herein use the name *C. griseoventris* to refer only to those specimens from Chiapas, unless specifically stated otherwise.

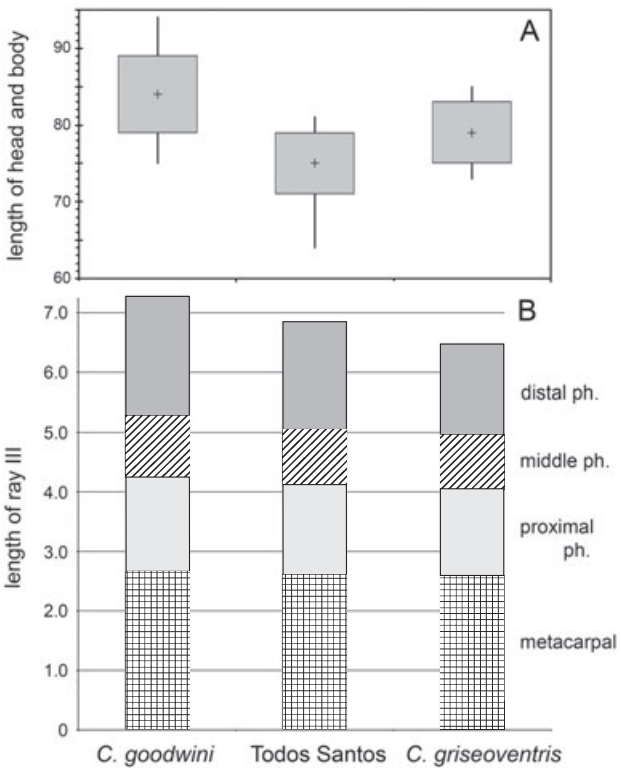

Figure 3. Comparison of body sizes with mean lengths of ray III of the manus among three populations of *Cryptotis*: A, box diagrams of head and body lengths (mm). Means represented by crosses (+); SDs by grey boxes; range limits by vertical lines. B, bar diagram comparing the mean lengths (mm) of bones comprising ray III. ph, phalanx.

RESULTS

Univariate variation

There is considerable variation among the three populations in the absolute proportions of individual metacarpals and phalanges (Tables 1, 2). *Cryptotis goodwini* has the largest average body size of the three populations (Fig. 3A) and the greatest average lengths of rays I, III, and V, and of each of the individual bones that comprise those rays (Fig. 3B). This species also averages the widest for each of the individual bones. All but the smallest individual *C. goodwini* can be distinguished from *C. griseoventris* and the Todos Santos population by the length of the distal phalanx and the widths of any of the four bones of ray III (Fig. 4). Although *C. griseoventris* is the second largest of the three groups in average body size, it has the shortest average total lengths of rays I, III, and V. Moreover, the average lengths and widths of almost all of the individual bones (except PPL of ray I and ML of ray V) are equal to or smaller than those of the Todos Santos population. Most individuals in these two populations can be distinguished

Table 1. Body size and lengths (mm) of bones and claws from three populations of *Cryptotis*

Taxon of *Cryptotis*	*N*	Head and body length (HB)	Metacarpal (ML)	Proximal phalanx (PPL)	Middle phalanx (MPL)	Distal phalanx (DPL)	Claw (CL)	Combined length (P2L/P3L)	Total length of ray (*TL*)
Ray I									
goodwini	16	**84** ± 5 75–94	**1.35** ± 0.08 1.22–1.47	**1.23** ± 0.12 1.01–1.50	–	**1.21** ± 0.09 1.00–1.35	**1.83** ± 0.17 1.37–2.08	**2.58** ± 0.17 2.29–2.95	**3.79** ± 0.22 3.41–4.31
Todos Santos	26	**75** ± 4 64–81 (*N* = 27)	**1.21** ± 0.08 1.08–1.46	**1.15** ± 0.08 0.96–1.34	–	**1.13** ± 0.05 0.97–1.24 (*N* = 24)	**1.98** ± 0.09 1.77–2.14	**2.36** ± 0.13 2.19–2.29	**3.49** ± 0.15 3.18–3.92
griseoventris	8	**79** ± 4 73–85	**1.20** ± 0.05 1.12–1.27	**1.18** ± 0.09 1.01–1.28	–	**1.05** ± 0.05 0.96–1.13	**1.91** ± 0.11 1.77–2.10	**2.38** ± 0.12 2.16–2.50	**3.43** ± 0.13 3.22–3.63
Ray III									
goodwini	14		**2.65** ± 0.10 2.49–2.84	**1.59** ± 0.10 1.41–1.82	**1.02** ± 0.10 0.89–1.16	**2.02** ± 0.08 1.90–2.18	**3.43** ± 0.21 3.11–3.76	**5.27** ± 0.21 4.96–5.66	**7.28** ± 0.27 6.89–7.84
Todos Santos	26		**2.59** ± 0.09 2.46–2.80	**1.53** ± 0.08 1.41–1.72	**0.92** ± 0.08 0.77–1.06	**1.80** ± 0.07 1.68–1.97 (*N* = 27)	**3.20** ± 0.13 2.92–3.43 (*N* = 27)	**5.05** ± 0.18 4.83–5.52	**6.84** ± 0.20 6.55–7.33
griseoventris	8		**2.59** ± 0.07 2.50–2.73	**1.46** ± 0.06 1.38–1.52	**0.90** ± 0.05 0.82–0.96	**1.52** ± 0.06 1.44–1.61	**2.79** ± 0.22 2.34–3.08	**4.95** ± 0.14 4.81–5.21	**6.47** ± 0.16 6.26–6.70
Ray V									
goodwini	15		**1.79** ± 0.09 1.64–1.94	**1.26** ± 0.06 1.14–1.41	**0.84** ± 0.06 0.72–0.92	**1.30** ± 0.08 1.18–1.48	**2.24** ± 0.20 2.03–2.73	**3.89** ± 0.15 3.66–4.20	**5.19** ± 0.18 4.96–5.67
Todos Santos	21		**1.67** ± 0.08 1.50–1.84 (*N* = 24)	**1.17** ± 0.10 0.87–1.41 (*N* = 24)	**0.76** ± 0.08 0.62–0.89	**1.12** ± 0.10 0.82–1.23 (*N* = 23)	**2.08** ± 0.20 1.29–2.33 (*N* = 23)	**3.59** ± 0.14 3.36–3.89	**4.71** ± 0.20 4.18–5.06
griseoventris	7		**1.68** ± 0.07 1.58–1.76	**1.13** ± 0.03 1.08–1.17	**0.76** ± 0.03 0.70–0.81	**0.95** ± 0.07 0.87–1.05	**1.76** ± 0.06 1.69–1.84 (*N* = 6)	**3.57** ± 0.09 3.47–3.68	**4.51** ± 0.06 4.40–4.58

Statistics are **mean** ± SD and total range. Variations in sample size are given in parentheses.

Table 2. Widths (mm) of bones and claws from three populations of *Cryptotis*

Taxon of *Cryptotis*	*N*	Metacarpal (MW)	Proximal phalanx (PPW)	Middle phalanx (MPW)	Distal phalanx (DPW)	Claw (CW)	Combined width (P2W/P3W)	Total width of all bones (TW)
Ray I								
goodwini	15	**0.49** ± 0.04 0.40–0.55	**0.43** ± 0.02 0.39–0.48	–	**0.61** ± 0.03 0.55–0.67	**0.36** ± 0.05 0.29–0.46 (*N* = 11)	**0.92** ± 0.05 0.81–1.00	**1.53** ± 0.06 1.41–1.64
Todos Santos	25	**0.38** ± 0.03 0.33–0.47	**0.34** ± 0.02 0.29–0.38	–	**0.50** ± 0.04 0.43–0.58	**0.28** ± 0.02 0.23–0.32 (*N* = 14)	**0.73** ± 0.04 0.62–0.81	**1.23** ± 0.07 1.07–1.36
griseoventris	8	**0.34** ± 0.03 0.29–0.37	**0.33** ± 0.04 0.30–0.38 (*N* = 4)	–	**0.46** ± 0.02 0.42–0.49	**0.26** ± 0.02 0.25–0.28 (*N* = 3)	**0.69** ± 0.04 0.64–0.73 (*N* = 4)	**1.16** ± 0.03 1.12–1.20
Ray III								
goodwini	14	**0.54** ± 0.03 0.49–0.58	**0.56** ± 0.02 0.53–0.60	**0.55** ± 0.03 0.52–0.62	**0.75** ± 0.04 0.65–0.80 (*N* = 13)	**0.57** ± 0.05 0.49–0.67 (*N* = 12)	**1.66** ± 0.05 1.54–1.74	**2.41** ± 0.06 2.28–2.49 (*N* = 13)
Todos Santos	26	**0.45** ± 0.02 0.40–0.50 (*N* = 22)	**0.46** ± 0.03 0.41–0.53 (*N* = 27)	**0.45** ± 0.03 0.39–0.49	**0.63** ± 0.04 0.56–0.71	**0.46** ± 0.03 0.42–0.51 (*N* = 8)	**1.35** ± 0.06 1.23–1.46 (*N* = 22)	**1.97** ± 0.08 1.83–2.12 (*N* = 22)
griseoventris	8	**0.40** ± 0.02 0.37–0.43	**0.41** ± 0.02 0.38–0.44	**0.41** ± 0.03 0.38–0.46	**0.56** ± 0.02 0.53–0.59	**0.42** ± 0.03 0.39–0.45 (*N* = 4)	**1.22** ± 0.06 1.15–1.32	**1.78** ± 0.07 1.70–1.91
Ray V								
goodwini	15	**0.55** ± 0.03 0.50–0.62	**0.44** ± 0.03 0.40–0.49	**0.48** ± 0.03 0.42–0.52	**0.57** ± 0.03 0.51–0.62 (*N* = 14)	**0.34** ± 0.03 0.30–0.42 (*N* = 12)	**1.48** ± 0.08 1.35–1.60 (*N* = 12)	**2.05** ± 0.09 1.91–2.16 (*N* = 14)
Todos Santos	21	**0.41** ± 0.03 0.37–0.48	**0.36** ± 0.02 0.32–0.40 (*N* = 24)	**0.36** ± 0.03 0.30–0.44	**0.45** ± 0.04 0.39–0.54	**0.29** ± 0.02 0.26–0.33 (*N* = 10)	**1.12** ± 0.06 1.02–1.27 (*N* = 19)	**1.58** ± 0.09 1.45–1.81 (*N* = 16)
griseoventris	7	**0.39** ± 0.04 0.34–0.43	**0.33** ± 0.02 0.28–0.35	**0.33** ± 0.03 0.28–0.36	**0.42** ± 0.02 0.40–0.46	0.25–0.28 (*N* = 2)	**1.04** ± 0.07 0.90–1.11	**1.47** ± 0.08 1.32–1.56

Statistics are **mean** ± SD and total range. Variations in sample size are given in parentheses.

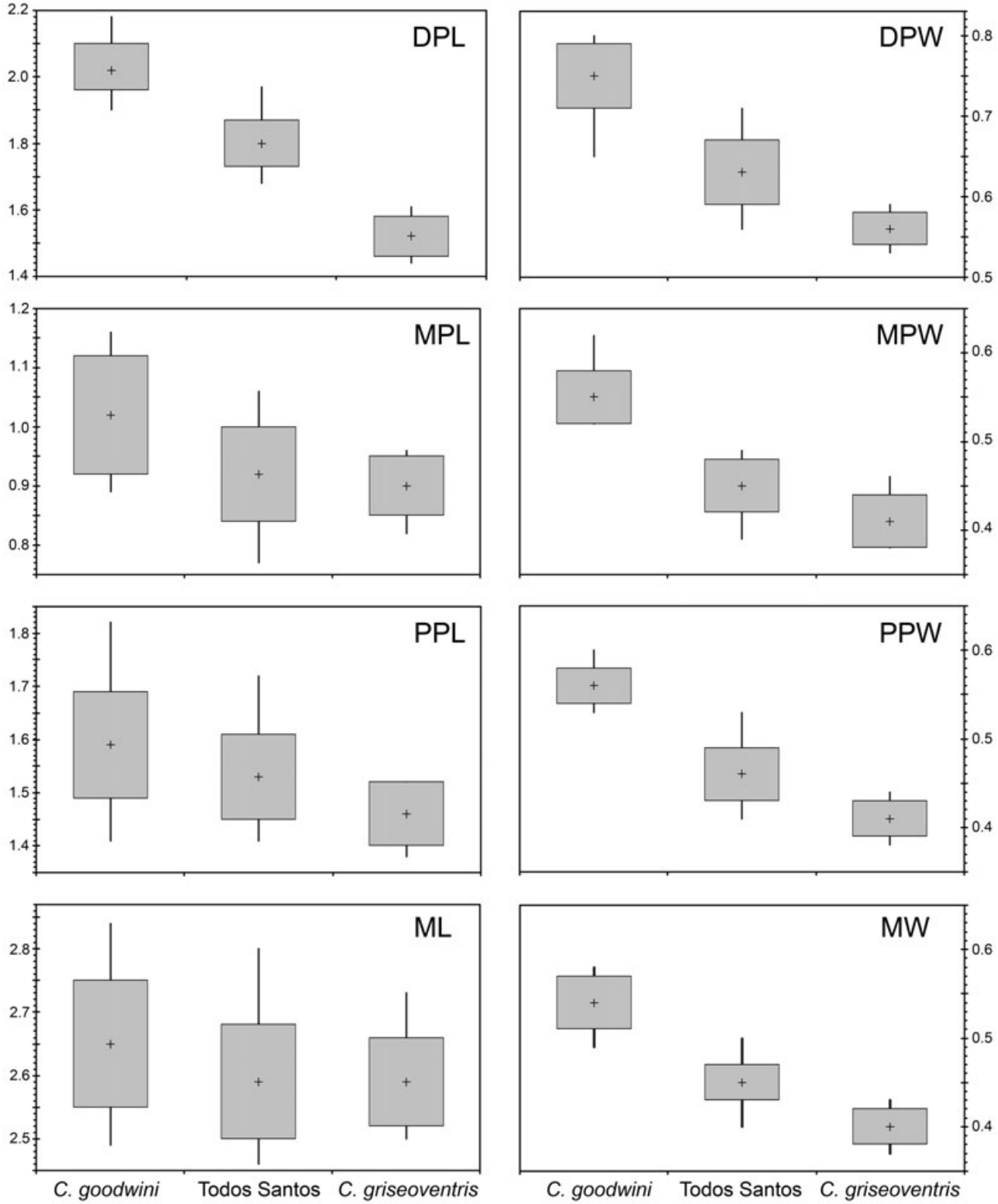

Figure 4. Box plots comparing lengths (left column) and widths (right) of bones from ray III of the manus of *Cryptotis*. Means represented by crosses (+); SDs by grey boxes; range limits by the vertical lines. DPL, length of distal phalanx; DPW, width of distal phalanx; ML, length of metacarpal; MPL, length of middle phalanx; MPW, width of middle phalanx; MW, width of metacarpal; PPL, length of proximal phalanx; PPW, width of proximal phalanx.

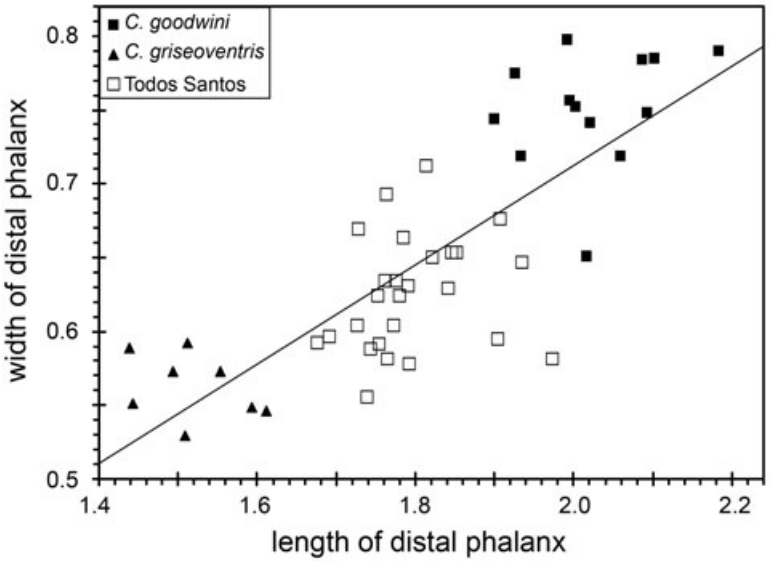

Figure 5. Plot of lengths and widths of distal phalanges from ray III of the manus of *Cryptotis*. Regression line ($y = 0.0343 + 0.3395x$) is based on data from all three populations.

by the widths of the metacarpal and the proximal and distal phalanges, and the length of the distal phalanx of ray III.

A bivariate plot of length and width of the distal phalanx completely segregates individuals into their a priori groupings (Fig. 5). This reflects the longer, broader distal phalanx of *C. goodwini*, and the shorter, narrower distal phalanx of *C. griseoventris*. The Todos Santos population is intermediate in size. A regression calculated for all three populations illustrates a general relationship of increasing width with length. Not surprisingly, this trend is mirrored by increasing width with length of the claw (not shown), but with greater overlap among the three groups. The relationship between length and width of the distal phalanx, however, is not completely linear among populations. Most specimens of *C. goodwini* and *C. griseoventris* plot very close to, or above, the regression line in Figure 5, whereas most specimens of the Todos Santos population plot below it. This relationship indicates that the Todos Santos population tends to have claws that are slightly narrower relative to their length, or that one or both of the other two populations tend to have somewhat wider claws than would be expected.

Percentages calculated by dividing by P2L or P3L for each of the bones indicate that metacarpals and proximal and middle phalanges generally contribute similarly to the lengths of the rays among the three populations (Table 3). The metacarpal generally constitutes approximately 50% of ray length in both ray I and ray III, despite the different numbers of phalanges. Compared to the other two populations, there is a tendency in *C. goodwini* toward reduction in relative length of the proximal phalanx in ray I and of the metacarpal in ray III. In ray V, the contribution of the metacarpal is always less than 50% of P3L. By contrast to the general similarity of the relative lengths of the metacarpals and proximal and middle phalanges among populations, the distal phalanges of all three rays are consistently longer in *C. goodwini* and the Todos Santos populations than in *C. griseoventris*.

The relative widths of the individual bones exhibit similar values among the bones comprising a particular ray within a population (Table 4). Mean widths of metacarpal, proximal phalanx, and middle phalanx in ray III of *C. griseoventris*, for example, are equal. The distal phalanx has the greatest relative width among all three rays in all three populations, but this variable was measured differently as a result of its unique, pyramidal shape (Fig. 2). Overall, *C. goodwini* has the relatively widest bones among the three populations, and there is a tendency for the bones of the Todos Santos population to be slightly wider on average than those of *C. griseoventris*, despite the former's smaller mean body size.

Division of the width of each bone by its length yielded proportions that provide additional contrasts among the three populations of shrews (Table 5). In general, the metacarpal, proximal phalanx, and middle phalanx of all three rays show tendencies to be relatively longest and narrowest in *C. griseoven-*

Table 3. Lengths (%) of bones and claws of rays I, III, and V relative to combined lengths of the two (P2L for ray I) or three most proximal bones (P3L) of the manus from three populations of *Cryptotis*

Taxon of *Cryptotis*	*N*	Metacarpal (ML)	Proximal phalanx (PPL)	Middle phalanx (MPL)	Distal phalanx (DPL)	Claw (CL)
Ray I						
goodwini	16	**53** ± 2	**47** ± 2	–	**47** ± 4	**71** ± 7
		49–56	44–51		39–54	57–86
Todos Santos	26	**51** ± 2	**49** ± 2	–	**48** ± 3	**84** ± 6
		48–57	43–52		40–54	68–96
						(*N* = 24)
griseoventris	8	**50** ± 2	**50** ± 2	–	**44** ± 3	**81** ± 6
		48–53	47–52		39–49	72–90
Ray III						
goodwini	14	**50** ± 1	**30** ± 1	**19** ± 2	**38** ± 1	**65** ± 4
		48–53	28–33	17–22	36–41	60–76
Todos Santos	26	**51** ± 1	**30** ± 1	**18** ± 1	**36** ± 2	**63** ± 2
		49–53	28–32	16–21	32–40	57–67
griseoventris	8	**52** ± 1	**29** ± 1	**18** ± 1	**31** ± 1	**56** ± 4
		51–54	29–30	17–19	29–32	48–62
Ray V						
goodwini	15	**46** ± 1	**32** ± 1	**22** ± 1	**34** ± 2	**58** ± 4
		44–49	31–34	19–24	29–37	52–65
Todos Santos	21	**47** ± 2	**32** ± 2	**21** ± 2	**31** ± 3	**58** ± 5
		44–50	26–35	18–25	25–34	38–64
griseoventris	7	**47** ± 1	**32** ± 1	**21** ± 1	**27** ± 2	**49** ± 2
		46–48	31–33	21–23	24–30	46–53
						(*N* = 6)

Statistics are **mean** ± SD and total range. Variations in sample size are given in parentheses.

tris, relatively shortest and widest in *C. goodwini*, and intermediate in the Todos Santos population. By contrast, the distal phalanx differs considerably among the rays. In ray I, *C. goodwini* has a relatively shorter, wider distal phalanx, whereas those of *C. griseoventris* and the Todos Santos population average the same. In rays III and V, the distal phalanges of *C. goodwini* and *C. griseoventris* average the same or almost the same, and they are shorter and wider than those of the Todos Santos population.

Variation within and among the fore feet

The unbiased coefficients of variation (*V**) calculated for HB for *C. goodwini*, *C. griseoventris*, and the Todos Santos population indicated relatively low variation in body size within each of these populations (Table 6) compared to a range of 4.3–8.0 calculated for seven other taxa in the genus *Cryptotis* (Woodman & Morgan, 2005). Among the variables measured from the manus of *C. goodwini*, *C. griseoventris*, and the Todos Santos population, half of the lengths had higher *V**s and all of the widths had much higher *V**s than those for HB among the three populations. If HB represents 'typical' variation within these populations, variation in the bones of the manus tended to be high. Comparisons among variables indicated that variation in widths of individual bones among the three populations of shrews (range 12.1–17.3) was always greater than variation in lengths (range 3.6–13.1). Moreover, *V**s for widths of individual bones were always greater among populations than within populations (range 3.3–11.5), but *V**s for lengths typically are not (range 2.4–10.5). Within a given population, there was a tendency for widths to be more variable than lengths, although the metacarpal was the only bone that consistently exhibited this pattern within each ray and within each population. Comparisons among the rays indicated that, overall, the bones of ray I tended to show the greatest variation within populations, and those of ray III exhibited the least. Among the three populations, the widths of the bones of ray III likewise tend to be less variable overall, although PPL and DPL from ray III were among the more variable length measures. The bones of ray V tended to be slightly more variable than those of ray I. Comparisons among individual elements revealed few obvious patterns. Within ray I, PPL was

Table 4. Width (%) of bones and claws of rays I, III, and V relative to combined lengths of the two (P2L) or three most proximal bones (P3L) of the manus from three populations of *Cryptotis*

Taxon of *Cryptotis*	*N*	Metacarpal (MW)	Proximal phalanx (PPW)	Middle phalanx (MPW)	Distal phalanx (DPW)	Claw (CW)
Ray I						
goodwini	15	**19** ± 2 15–22	**17** ± 1 15–20	–	**23** ± 1 21–25	**14** ± 2 11–17 (*N* = 11)
Todos Santos	25	**16** ± 2 13–22	**15** ± 1 12–16	–	**21** ± 2 18–25 (*N* = 26)	**12** ± 1 10–14 (*N* = 14)
griseoventris	8	**14** ± 1 12–15	**13** ± 1 12–15 (*N* = 4)	–	**20** ± 1 17–22	**11** ± 1 11–12 (*N* = 3)
Ray III						
goodwini	14	**10** ± 1 9–12	**11** ± 0.5 10–11	**10** ± 1 10–12	**14** ± 1 13–16 (*N* = 13)	**11** ± 1 9–12 (*N* = 12)
Todos Santos	26	**9** ± 1 8–10 (*N* = 22)	**9** ± 1 8–10	**9** ± 1 8–10	**12** ± 1 11–14	**9** ± 1 8–10 (*N* = 8)
griseoventris	8	**8** ± 0.5 7–9	**8** ± 0.5 8–9	**8** ± 0.5 8–9	**11** ± 0.5 11–12	**8** ± 1 8–9 (*N* = 4)
Ray V						
goodwini	15	**14** ± 1 12–16	**11** ± 1 10–13	**12** ± 1 11–13	**15** ± 1 14–16 (*N* = 14)	**9** ± 1 8–10 (*N* = 12)
Todos Santos	21	**11** ± 1 10–13 (*N* = 19)	**10** ± 1 9–11	**10** ± 1 8–11	**13** ± 1 11–15 (*N* = 19)	**8** ± 1 7–9 (*N* = 10)
griseoventris	7	**11** ± 1 10–12	**9** ± 1 8–10	**9** ± 1 8–10	**12** ± 0.5 11–12	**7–8** (*N* = 2)

Statistics are **mean** ± SD and total range. Variations in sample size are given in parentheses.

consistently the most variable length measurement both within and among populations, whereas MW had the most variable width. In ray III, ML was the least variable length and MPL was the most variable, whereas, in ray V, ML and PPL were consistently the two least variable lengths. In neither ray III nor V were there any consistent patterns of variation in width among the bones. These patterns of variation provide some indication of the usefulness of width variables both for grouping individuals from the same populations and for distinguishing individuals from different populations in our subsequent analyses.

Correlations within and among the fore feet

In the correlation matrix calculated for all variables among all three populations, none of the fore foot variables correlated strongly with HB (Appendix I). More striking is the fact that none of the length variables from individual bones correlated strongly with any other length or width variables, a primary exception being DPL from rays III and V. These two variables correlated strongly with each other and with most width variables from rays III and V, but not with those from ray I. Similar to the length variables from individual bones, P3L from all three rays and TL from ray I exhibited few strong correlations among the other variables. By contrast, TL from ray III had strong correlations with DPL and with most width variables from both rays III and V. TL from ray V correlated with DPL from those two rays and with most width variables from all three rays.

By contrast to most length variables, all of the width variables from the bones (but not claws) within and among rays correlated strongly with one another. In addition, CW of ray III correlated with DPL, with

Table 5. Width (%) relative to length of bones and claws of rays I, III, and V of the manus from three populations of *Cryptotis*

Taxon of *Cryptotis*	*N*	Metacarpal (MW)	Proximal phalanx (PPW)	Middle phalanx (MPW)	Distal phalanx (DPW)	Claw (CW)
Ray I						
goodwini	15	**36** ± 4 29–43	**35** ± 3 31–41	–	**51** ± 4 43–58	**20** ± 3 16–26 (*N* = 11)
Todos Santos	26	**31** ± 4 25–44	**30** ± 3 24–38 (*N* = 25)	–	**44** ± 4 39–55	**14** ± 1 12–17 (*N* = 14)
griseoventris	8	**29** ± 3 23–32	**26** ± 3 24–30 (*N* = 4)	–	**44** ± 2 41–48	**14** ± 1 13–15 (*N* = 3)
Ray III						
goodwini	14	**21** ± 1 18–23	**36** ± 2 32–40	**55** ± 6 45–66	**37** ± 2 32–40 (*N* = 13)	**17** ± 2 14–19 (*N* = 12)
Todos Santos	26	**17** ± 1 15–20 (*N* = 22)	**30** ± 2 25–36	**50** ± 5 37–60	**35** ± 2 29–39	**15** ± 1 13–17 (*N* = 8)
griseoventris	8	**15** ± 1 14–17	**28** ± 1 27–30	**46** ± 4 41–50	**37** ± 2 34–41	**15** ± 2 14–18 (*N* = 4)
Ray V						
goodwini	15	**31** ± 2 27–36	**35** ± 3 31–40	**57** ± 5 50–72	**44** ± 3 38–49 (*N* = 14)	**15** ± 2 13–18 (*N* = 12)
Todos Santos	20	**24** ± 2 22–29 (*N* = 20)	**31** ± 3 25–38	**48** ± 7 34–62 (*N* = 21)	**41** ± 3 36–47	**15** ± 4 12–24 (*N* = 10)
griseoventris	7	**23** ± 2 20–27	**29** ± 2 26–31	**43** ± 3 38–48	**45** ± 4 40–53	**13–17** (*N* = 2)

Statistics are **mean** ± SD and total range. Variations in sample size are given in parentheses.

all of the width variables from that ray, with DPL of ray V, and with many of the width variables from rays I and V. These correlations suggest widening of the claw on ray III is associated with lengthening of the distal phalanx and widening of all of the bones of the ray. On ray V, DPL was correlated with several width variables on that ray; CL was correlated with CW; and CW was correlated with MPW and MW. Hence, there is a tendency for the distal phalanx on ray V to elongate and widen as the bones of that ray become wider, although not all of the relationships were as clear and strong as in ray III.

It appeared from the correlation matrix that any modification in length of a given bone (except the distal phalanx) is mostly independent of any other modification in the fore foot. By contrast, the strong correlations among width variables of the various bones indicates that widening of those bones may be occurring in concert. Moreover, on rays III and V (but not ray I), the length of the distal phalanx and total length of the ray appear to increase with the widening of the metacarpals and phalanges. There also is a strong tendency for the claw on ray III to widen as the bones of the fore foot widen. The claw of ray III lengthens as well, although this was correlated with the lengthening of the distal phalanx rather than the widening of any bone. Similar to ray III, the claw of ray V lengthens with its distal phalanx. Although raw measurements of the distal phalanx of ray I suggested the same pattern of lengthening among populations, neither it nor the length of the claw were strongly correlated with broadening of any elements. Widening of the bones of the manus and lengthening of the claws represent general trends among all populations, occurring without respect to body size.

Table 6. Unbiased coefficients of variation (V^*) for variables from three populations of *Cryptotis*

Taxon of *Cryptotis*	HB	ML	PPL	MPL	DPL	CL	P2L/P3L	TL	MW	PPW	MPW	DPW	CW
Ray I													
goodwini	5.8	5.9	9.8	–	7.8	9.6	6.8	6.0	8.5	5.8	–	5.8	14.8
Todos Santos	5.1	6.5	7.2	–	4.8	4.6	5.5	4.3	9.0	5.5	–	7.3	8.3
griseoventris	5.0	4.3	8.1	–	4.6	6.0	5.3	3.9	8.5	11.5	–	5.2	7.0
Totals	7.5	8.0	8.6	–	7.5	7.4	17.9	6.3	16.0	13.2	–	12.5	17.8
Ray III													
goodwini		4.0	6.1	10.4	4.0	6.3	4.0	3.7	4.8	3.3	4.8	5.4	8.2
Todos Santos		3.6	5.3	8.8	4.0	4.1	3.5	2.9	5.5	7.2	5.6	6.3	6.9
griseoventris		2.8	4.2	6.3	4.3	8.1	2.9	2.5	5.3	4.9	7.5	4.1	6.4
Totals		3.6	5.9	10.4	10.0	8.2	8.3	5.2	12.6	13.1	12.1	11.8	14.9
Ray V													
goodwini		4.9	5.0	7.3	6.5	8.9	3.9	3.5	5.9	6.5	5.7	5.1	10.2
Todos Santos		5.0	8.4	10.5	8.6	9.6	4.0	4.3	8.2	6.2	8.4	9.2	8.4
griseoventris		4.1	2.4	4.6	7.3	3.8	2.7	1.4	9.5	7.2	10.1	4.2	10.2
Totals		5.4	7.9	9.7	13.1	11.4	11.3	6.6	17.3	13.4	16.7	14.3	13.3

CL, length of claw; CW, width of claw; DPL, length of distal phalanx; DPW, width of distal phalanx; HB, length of head and body; ML, length of metacarpal; MPL, length of middle phalanx; MPW, width of middle phalanx; MW, width of metacarpal; P2L, length of proximal two bones (= ML + PPL); P3L, length of proximal three bones (= ML + PPL + MPL); PPL, length of proximal phalanx; PPW, width of proximal phalanx.

Table 7. Comparative phalangeal indices (PI) for rays I, III, and V of the manus from three populations of *Cryptotis*

	Ray I	Ray III	Ray V
Cryptotis goodwini	**91** ± 7	**99** ± 5	**118** ± 6
	79–104	88–109	102–125
	(N = 16)	(N = 16)	(N = 15)
Todos Santos	**95** ± 8	**95** ± 3	**115** ± 7
	76–108	89–103	101–125
	(N = 26)	(N = 26)	(N = 21)
Cryptotis griseoventris	**99** ± 7	**91** ± 3	**112** ± 4
	88–109	85–96	108–120
	(N = 8)	(N = 8)	(N = 7)

Statistics are **mean** ± SD, total range, and sample sizes.

Phalangeal index and relative ray length

Average PIs calculated for rays I and III among the three populations were in the range 91–99%, whereas those for ray V were in the range 112–118% (Table 7). For ray I, the index was highest for *C. griseoventris* and lowest for *C. goodwini*, whereas for rays III and V, the rankings were reversed. Higher PIs indicate longer digits (i.e. PPL + MPL) relative to metacarpals, hence *C. goodwini* averaged the longest digits on rays III and V, and the shortest on ray I. For all three rays, the digits of the Todos Santos population averaged intermediate in length.

PI typically varies considerably among rays of an individual species (Lemelin, 1999), and the PI of ray III is most commonly used for comparisons. There also may be a considerable phylogenetic component to this index (Weisbecker & Schmid, 2007). In general, however, a high PI tends to be associated with greater arboreality and grasping of small-diameter supports (Lemelin, 1999; Weisbecker & Schmid, 2007; Kirk *et al.*, 2008). The average values for the three shrew populations exhibited a relatively narrow distribution that is generally within the range for terrestrial mammals in contrast to arboreal mammals (Lemelin, 1999; Kirk *et al.*, 2008).

The relative contributions of the metacarpal, proximal phalanx, and middle phalanx to the length (P3L) of ray III are almost identical among *C. goodwini*, *C. griseoventris*, and the Todos Santos population, and do not serve to distinguish the three populations (Table 3). Mapping these values onto Kirk *et al.*'s (2008) ternary diagrams of different groupings of Primates, Carnivora, Dermoptera, Rodentia, Scandentia, and Metatherians, functionally associates the three shrews most closely with terrestrial sciurid and non-sciurid rodents and three species of terrestrial tree shrews.

The total lengths of rays I and V relative to ray III were almost the same among all three populations of shrews (Table 1). Ray I averaged 52% the length of ray III among *C. goodwini* (±2; N = 11), 53% in *C. griseoventris* (±2; N = 8), and 51% in the Todos Santos population (±1; N = 15). The respective average lengths of ray V relative to ray III were 72% for *C. goodwini* (±2; N = 10), 70% for *C. griseoventris*

Table 8. Factor loadings for the first three axes from a principal components (PC) analysis (Fig. 6) of seven log-transformed variables from ray III of the manus from three populations of *Cryptotis*

	Correlations		
Variable	PC I	PC II	PC III
DPW	0.930	0.129	0.103
MPW	0.912	0.167	0.117
PPW	0.902	0.241	0.106
DPL	0.882	0.208	0.044
PPL	0.675	–0.517	0.333
MPL	0.558	0.105	–0.789
ML	0.496	–0.773	–0.243
Eigenvalue	4.302	1.021	0.831
Variation explained (%)	61.5	14.6	11.9

DPL, length of distal phalanx; DPW, width of distal phalanx; ML, length of metacarpal; MPL, length of middle phalanx; MPW, width of middle phalanx; MW, width of metacarpal; PPL, length of proximal phalanx; PPW, width of proximal phalanx.

(±2; $N = 7$), and 69% for the Todos Santos population (±3; $N = 14$). In more derived fossorial talpids, the rays generally tend to be more similar in length, whereas, in more primitive talpids, such as *Uropsilus*, there is greater variation among the rays (Reed, 1951; Sánchez-Villagra & Menke, 2005). The large differences among the three rays in the shrews that we studied are most similar to primitive, less fossorial moles.

Multivariate analysis

In our PCA of seven log-transformed measurements from ray III, all variables contributed strongly and positively to factor 1 (Table 8), indicating that this axis is a reasonable representation of overall size of ray III and, by extension, the size of the manus. The three width variables had the highest correlations on this axis, followed by the length of the distal phalanx, again emphasizing the contributions of trends of increasing widths of all bones and lengthening of the distal phalanx to variation among the three populations. Two length variables (ML, PPL) contributed strongly and negatively to factor 2, such that higher scores represent shorter metacarpals and proximal phalanges. The third factor axis most strongly represented a negatively-weighted MPL, such that higher scores on this axis indicate shorter middle phalanges.

A plot of scores on the first two factor axes serves to illustrate the distinctiveness of the three populations of shrews and to highlight morphological trends within and among the populations (Fig. 6). All three populations are completely separated by the combination of factors 1 and 2. Although the Todos Santos population overlaps both *C. goodwini* and *C. griseoventris* along factor 1 axis, this factor contributes most to the separation of the three populations and illustrates a distinct trend of increasing size of ray III from the smallest (*C. griseoventris*) to the largest (*C. goodwini*). The three populations are inseparable on factor 2 axis alone, but the combination of factors 1 and 2 results in their distribution as three distinct groups without overlap. A similar pattern is exhibited by a plot of factor 1 and factor 3 (not shown). Similar to factor 2, factor 3 by itself contributes little to any separation among populations. In combination with factor 1, however, the three populations form cohesive, recognizable groupings, although with some overlap between adjacent groups.

Within each of the three populations, there is a tendency for individuals with a larger ray III (i.e. factor 1) to have a longer metacarpal and proximal phalanx (factor 2). This is opposite the trend among populations, in which the metacarpal and proximal phalanx become relatively shorter as the overall size of ray III increases. A similar distribution is exhibited when factor 3 is plotted against factor 1 (not shown), indicating that similar relationships within and among populations exist between length of the middle phalanx and size of ray III. In absolute terms, the actual values for lengths of the metacarpal and the proximal and middle phalanges are relatively similar among the three populations despite differences in body size, whereas the widths of the bones vary considerably among populations (Tables 1, 2).

Backward stepwise and forward stepwise discriminant function analyses both resulted in the same model utilizing four variables (DPL, DPW, PPL, PPW). Plots of canonical scores from the the two analyses are the same (Fig. 7); both separate the three populations into three distinct groups without obvious overlap. The resulting classification and jackknifed classification functions both classified all but one specimen into their a priori populations. An individual of the Todos Santos population from Aldea El Rancho was misclassified as a *C. goodwini* in each case. This specimen plots on the periphery of the distribution of the Todos Santos population in Figure 7. Other specimens from Aldea El Rancho were classified as members of the Todos Santos population. We consider this specimen a member of that population, although its misclassification is indicative of the close morphological relationships between the two populations.

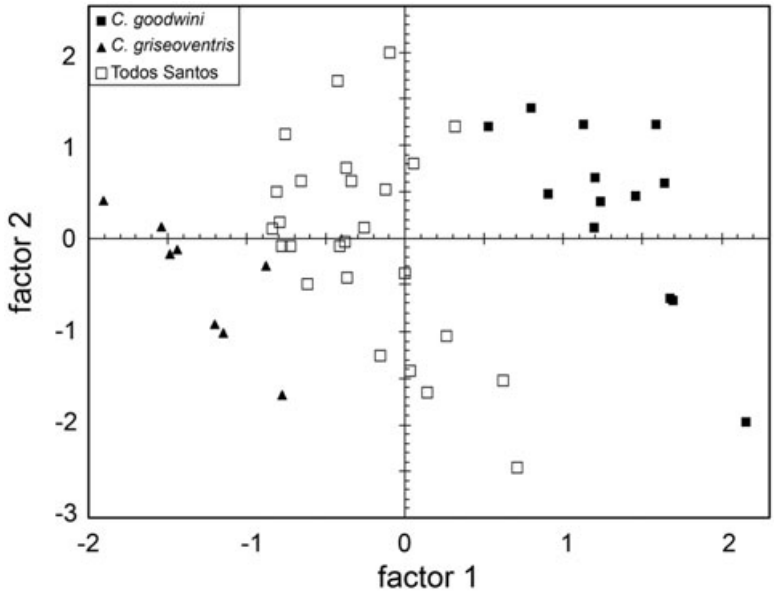

Figure 6. Plot of factor scores for three populations of *Cryptotis* on the first two axes from a principal components analysis of five log-transformed variables from ray III of the manus (Table 8).

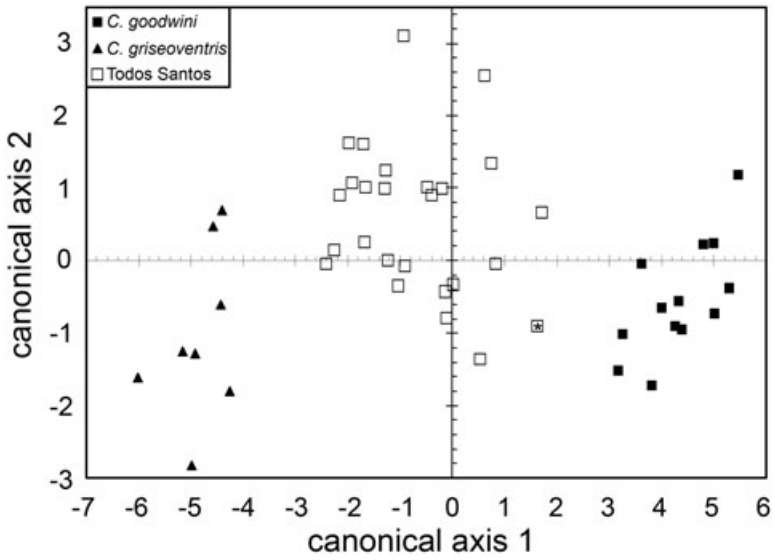

Figure 7. Plot of scores for three populations of *Cryptotis* on canonical axes 1 and 2 from backward stepwise discriminant function analysis of seven log-transformed variables from ray III of the manus. One Todos Santos specimen misclassified as *Cryptotis goodwini* is marked with an asterisk.

DISCUSSION

The fore feet of *C. goodwini*, *C. griseoventris*, and the sample from Todos Santos all exhibit the general structure identified previously among other members of the *C. mexicana* group (Woodman & Morgan, 2005). The fore feet are enlarged relative to most other members of the genus *Cryptotis*, and they bear long, broad claws. Internally, the metacarpals and proximal and middle phalanges are relatively short and wide, whereas the distal phalanx is elongate and wide (Fig. 1). Morphologies of the fore feet among the three populations fit with a general pattern of gradual enlargement that has been recognized among species of the *C. mexicana* group (Woodman & Timm, 1999, 2000). Relationships of the changes in the elements of

the fore feet, however, are not simple gradations among species. For example, the regression of width and length of the distal phalanx (Fig. 5) indicates that the relationship between these two variables is not completely linear among the three populations. Similarly, variation in the manus is not correlated with body size, as originally considered (Woodman & Timm, 1999). Among our samples, the population with the smallest fore feet (shortest total lengths of rays; shortest, narrowest claws; relatively longest, narrowest metacarpals and proximal and middle phalanges) was of intermediate body size, whereas the population with the smallest body size had fore feet of intermediate size. These variations from the trend illustrate the individual evolutionary trajectories among these species despite their commonalities in general structural pattern.

Most variation among populations is in widths of the bones in all three rays. In addition, there is considerable variation among populations in lengths of the distal phalanges of rays III and V. There are weaker trends toward the shortening of the metacarpal and proximal and middle phalanges of ray III, as these same bones increase in width. As noted previously, these trends are similar to trends that mark increased fossorial specialization in the Talpidae, and it has been hypothesized that they mark different degrees of dependence upon burrowing among different species of *Cryptotis* (Woodman & Timm, 1999). If the increased length and breadth of the distal phalanges and the relative shortening and broadening of the other rays are adaptations to increased digging efficiency, a greater emphasis appears to be placed on the middle and lateral rays than on the medial ray in these shrews.

ACKNOWLEDGEMENTS

We thank Walter Bulmer, Ralph Eckerlin, Jack Matson, and Nicté Ordónez for providing new specimens of *Cryptotis* from Guatemala. Franklin Herrera assisted with permits for field work in Guatemala. R. Terry Chesser, Sandy Feinstein, Robert D. Fisher, and two anonymous reviewers provided valuable input on previous versions of this manuscript. Ryan Stephens was supported by the Bill and Jean Lane Internship Endowment of the Research Training Program, National Museum of Natural History, Washington. Any use of trade, product, or firm names is for descriptive purposes only and does not imply endorsement by the US government.

REFERENCES

Goldman EA. 1951. Biological investigations in Mexico. *Smithsonian Miscellaneous Collections* **115:** i–xiii, 1–476.

Jackson HHT. 1933. Five new shrews of the genus *Cryptotis* from Mexico and Guatemala. *Proceedings of the Biological Society of Washington* **46:** 79–82.

Kirk EC, Lemelin P, Hamrick MW, Boyer DM, Bloch JI. 2008. Intrinsic hand proportions of euarchontans and other mammals: implications for the locomotor behavior of plesiadapiforms. *Journal of Human Evolution* **55:** 278–299.

Lemelin P. 1999. Morphological correlates of substrate use in didelphid marsupials: implications for primate origins. *Journal of Zoology* **247:** 165–175.

Reed CA. 1951. Locomotion and appendicular anatomy in three soricoid insectivores. *American Midland Naturalist* **45:** 513–671.

Sánchez-Villagra MR, Menke PR. 2005. The mole's thumb – evolution of the hand skeleton in talpids (Mammalia). *Zoology* **108:** 3–12.

Sokal RR, Rohlf FJ. 1981. *Biometry*, 2nd edn. New York, NY: WH Freeman and Company.

Weisbecker V, Schmid S. 2007. Autopodial skeletal diversity in hystricognath rodents: functional and phylogenetic aspects. *Mammalian Biology* **72:** 27–44.

Woodman N. 2005. Evolution and biogeography of Mexican small-eared shrews of the *Cryptotis mexicana*-group (Insectivora: Soricidae). In: Sánchez-Cordero V, Medellín RA, eds. *Contribuciones Mastozoológicas en Homenaje a Bernardo Villa*. Mexico City: Universidad Nacional Autónoma de México and CONABIO, 523–534.

Woodman N, Croft DA. 2005. Fossil shrews from Honduras and their significance for late glacial evolution in body size (Mammalia: Soricidae: *Cryptotis*). *Fieldiana, Geology, New Series* **51:** 1–30.

Woodman N, Morgan JJP. 2005. Skeletal morphology of the forefoot in shrews (Mammalia: Soricidae) of the genus *Cryptotis*, as revealed by digital x-rays. *Journal of Morphology* **266:** 60–73.

Woodman N, Pefaur J. 2008. Order Soricomorpha Gregory, 1910. In: Gardner AL, ed. *Mammals of South America*, Vol. I: marsupials, xenarthrans, shrews, and bats. Chicago, IL: University of Chicago Press, 177–187 [title page incorrectly gives publication year as 2007].

Woodman N, Timm RM. 1999. Geographic variation and evolutionary relationships among broad-clawed shrews of the *Cryptotis goldmani*-group (Mammalia: Insectivora: Soricidae). *Fieldiana, Zoology, New Series* **91:** 1–35.

Woodman N, Timm RM. 2000. Taxonomy and evolutionary relationships of Phillips' small-eared shrew, *Cryptotis phillipsii* (Schaldach, 1966), from Oaxaca, Mexico (Mammalia: Insectivora: Soricidae). *Proceedings of the Biological Society of Washington* **113:** 339–355.

APPENDIX I

CORRELATION MATRIX

Pairwise Pearson's correlations of untransformed variables from rays I, III, and V of the manus from three populations of *Cryptotis*. Correlations > 0.75 are shown in bold. Abbreviations of variables are defined in the Material and methods; the numeral before a variable indicates the ray with which it is associated.

	HB	1CL	1CW	1DPL	1DPW	1PPL	1PPW	1ML	1MW	1P3L	1totL
HB	1.000										
1CL	–0.497	1.000									
1CW	0.597	–0.215	1.000								
1DPL	0.140	0.315	0.465	1.000							
1DPW	0.517	–0.226	0.669	0.613	1.000						
1PPL	0.309	0.134	0.575	0.375	0.405	1.000					
1PPW	0.577	–0.334	**0.814**	0.516	**0.783**	0.456	1.000				
1ML	0.433	–0.257	0.593	0.403	0.675	0.491	0.680	1.000			
1MW	0.537	–0.362	0.610	0.462	**0.830**	0.289	**0.779**	0.487	1.000		
1P3L	–0.178	0.137	0.122	0.138	0.181	0.318	0.124	0.256	0.217	1.000	
1totL	0.384	0.058	0.670	0.725	0.706	**0.807**	0.699	**0.818**	0.516	0.315	1.000
3CL	0.168	0.085	0.499	0.602	0.654	0.286	0.543	0.386	0.582	0.273	0.528
3CW	0.545	–0.182	0.623	0.685	**0.835**	0.303	0.742	0.625	**0.796**	0.233	0.680
3DPL	0.397	–0.212	0.654	0.668	**0.767**	0.280	0.721	0.574	0.723	0.185	0.634
3DPW	0.455	–0.287	0.681	0.577	**0.867**	0.442	**0.852**	0.711	**0.785**	0.305	0.724
3MPL	0.416	–0.064	0.404	0.459	0.551	0.495	0.434	0.400	0.401	0.174	0.574
3MPW	0.522	–0.339	0.711	0.549	**0.775**	0.329	**0.873**	0.550	**0.834**	0.223	0.591
3PPL	0.262	–0.194	0.601	0.198	0.583	0.434	0.576	0.579	0.556	0.522	0.528
3PPW	0.488	–0.312	0.652	0.607	**0.831**	0.275	**0.820**	0.543	**0.872**	0.222	0.588
3ML	0.270	–0.127	0.450	0.134	0.179	0.538	0.432	0.534	0.242	0.394	0.527
3MW	0.447	–0.309	0.647	0.641	**0.851**	0.248	**0.840**	0.617	**0.850**	0.221	0.620
3P3L	0.223	–0.227	0.414	0.240	0.341	0.270	0.373	0.467	0.237	0.294	0.420
3totL	0.458	–0.215	0.686	0.561	0.740	0.536	0.740	0.702	0.681	0.382	**0.764**
5CL	0.182	–0.026	0.559	0.480	0.544	0.186	0.499	0.271	0.520	0.225	0.388
5CW	0.599	–0.282	0.676	0.398	0.720	0.475	0.733	**0.828**	0.606	0.262	0.700
5DPL	0.421	–0.231	0.729	0.626	0.716	0.301	0.729	0.476	0.726	0.191	0.583
5DPW	0.611	–0.369	0.723	0.508	**0.834**	0.439	**0.824**	0.674	**0.795**	0.258	0.695
5MPL	0.424	–0.434	0.326	0.196	0.539	0.209	0.381	0.523	0.362	0.005	0.399
5MPW	0.592	–0.270	0.659	0.505	**0.816**	0.434	**0.851**	0.680	**0.849**	0.224	0.684
5PPL	0.190	–0.126	0.738	0.438	0.533	0.349	0.561	0.388	0.471	0.243	0.492
5PPW	0.557	–0.367	0.649	0.518	**0.752**	0.345	**0.835**	0.656	**0.819**	0.166	0.640
5ML	0.357	–0.162	0.587	0.343	0.538	0.537	0.509	0.704	0.367	0.212	0.689
5MW	0.619	–0.322	0.722	0.569	**0.783**	0.381	**0.904**	0.687	**0.790**	0.137	0.691
5P3L	0.261	–0.235	0.450	0.343	0.499	0.224	0.459	0.450	0.356	0.192	0.431
5totL	0.563	–0.263	**0.807**	0.570	**0.824**	0.481	**0.758**	0.683	0.735	0.265	0.734

	3CL	3CW	3DPL	3DPW	3MPL	3MPW	3PPL	3PPW	3ML	3MW	3P3L	3totL
3CL	1.000											
3CW	0.648	1.000										
3DPL	**0.801**	**0.777**	1.000									
3DPW	0.625	**0.761**	**0.805**	1.000								
3MPL	0.583	0.464	0.537	0.486	1.000							
3MPW	0.596	**0.767**	**0.787**	**0.868**	0.427	1.000						
3PPL	0.435	0.456	0.533	0.606	0.227	0.493	1.000					
3PPW	0.687	**0.867**	**0.818**	**0.835**	0.452	**0.877**	0.490	1.000				
3ML	0.309	0.239	0.294	0.330	0.325	0.343	0.531	0.275	1.000			
3MW	0.653	**0.820**	**0.817**	**0.874**	0.425	**0.883**	0.518	**0.925**	0.183	1.000		
3P3L	0.197	0.502	0.326	0.631	0.316	0.562	0.376	0.276	**0.812**	0.241	1.000	

APPENDIX I *Continued*

	3CL	3CW	3DPL	3DPW	3MPL	3MPW	3PPL	3PPW	3ML	3MW	3P3L	3totL
3totL	**0.770**	0.713	**0.877**	**0.801**	0.697	0.749	0.733	**0.753**	0.640	0.728	**0.912**	1.000
5CL	0.727	0.521	0.709	0.597	0.289	0.527	0.444	0.599	0.213	0.598	0.415	0.616
5CW	0.463	0.745	0.711	**0.752**	0.488	0.599	0.586	0.651	0.443	0.641	0.655	0.738
5DPL	0.732	**0.838**	**0.848**	0.732	0.444	0.707	0.488	**0.762**	0.290	**0.761**	0.539	**0.761**
5DPW	0.665	0.743	**0.802**	**0.869**	0.571	**0.811**	0.579	**0.812**	0.424	**0.799**	0.691	**0.831**
5MPL	0.287	0.173	0.452	0.438	0.492	0.337	0.194	0.431	0.041	0.403	0.328	0.431
5MPW	0.626	**0.784**	**0.773**	**0.846**	0.504	**0.860**	0.552	**0.835**	0.405	**0.846**	0.646	**0.788**
5PPL	0.472	0.675	0.593	0.586	0.267	0.555	0.570	0.520	0.181	0.588	0.445	0.573
5PPW	0.672	**0.820**	**0.801**	**0.794**	0.531	**0.863**	0.518	**0.839**	0.516	**0.797**	0.689	**0.822**
5ML	0.322	0.666	0.413	0.467	0.299	0.426	0.499	0.470	0.478	0.539	0.377	0.552
5MW	0.558	**0.759**	0.742	**0.852**	0.524	**0.864**	0.466	**0.800**	0.435	**0.804**	0.456	**0.762**
5P3L	0.304	0.601	0.388	0.545	0.329	0.521	0.380	0.432	0.276	0.368	**0.824**	0.628
5totL	0.696	**0.837**	**0.822**	**0.798**	0.526	0.722	0.628	**0.792**	0.363	**0.794**	0.668	**0.825**

	5CL	5CW	5DPL	5DPW	5MPL	5MPW	5PPL	5PPW	5ML	5MW	5P3L	5totL
5CL	1.000											
5CW	0.397	1.000										
5DPL	**0.827**	0.636	1.000									
5DPW	0.641	0.705	**0.824**	1.000								
5MPL	0.108	0.563	0.181	0.456	1.000							
5MPW	0.547	**0.760**	0.720	**0.870**	0.447	1.000						
5PPL	0.693	0.381	0.662	0.613	0.229	0.592	1.000					
5PPW	0.564	0.738	**0.775**	**0.851**	0.439	**0.881**	0.509	1.000				
5ML	0.387	0.645	0.499	0.579	0.251	0.602	0.502	0.539	1.000			
5MW	0.450	**0.763**	0.679	**0.856**	0.387	**0.872**	0.451	**0.883**	0.510	1.000		
5P3L	0.584	0.707	0.622	**0.794**	0.611	0.727	0.685	0.607	0.476	0.495	1.000	
5totL	**0.770**	0.735	**0.872**	**0.895**	0.470	**0.806**	**0.846**	**0.800**	**0.767**	0.724	**0.926**	1.000

APPENDIX II

Specimens examined

Specimens and catalog numbers are from the Division of Mammals, National Museum of Natural History, Washington, DC (USNM), except for one specimen from the University of Michigan Museum of Zoology, Ann Arbor (UMMZ).

Cryptotis goodwini (16): Guatemala: Quetzaltenango: Calel, 10 200 feet (type series: 77070, 77072, 77073, 77075–77084). Quezaltenango: Volcán Santa María, 9000–11 000 feet (77086, 77087). San Marcos: Finca La Paz, 1200 m (UMMZ 103416).

Cryptotis griseoventris (8): Mexico: Chiapas: San Cristóbal de las Casas, 8000–9500 feet (type series: 75886–75893).

Todos Santos [*Cryptotis griseoventris*] (27). Guatemala: Huehuetenango: Todos Santos Cuchumatán (77051–77064, 77066–77068); Hacienda Chancol, 9500–11 000 feet (77069); Laguna Magdalena, 2925 m (569554, 569555, 570337, 570340); Puerto al Cielo, 3350 m (570248); Aldea El Rancho, 3020 m (570256, 570257, 570313, 570314).

